ON THE RELIABILITY OF CIRCULATION MODELS

by

T.J. Simons

National Water Research Institute
Canada Centre for Inland Waters
Burlington, Ontario
Canada L7R 4A6

EXECUTIVE SUMMARY

Hydrodynamic models appear to have been generally accepted as useful tools to elucidate the dynamics of lake and ocean circulations and to simulate short-term local current patterns as well as climatological mass transports in lakes and oceans. Unlike their meteorological counterparts which have been constantly improved by recourse to routine observations from a dense network of weather stations, oceanic circulation models cannot be adequately verified with the available data base and their acceptance is based more on faith than fact. There is no indication that this faith has been shaken by the conclusions of systematic verification studies of hydrodynamic models of the Great Lakes which raise serious doubts about the ability of such models to simulate long-term circulation patterns. Perhaps it is felt that the disparity of oceanic and limnological scales or differences in dynamical processes render a comparison of circulation models of lakes and oceans invalid.

Long time series current meter observations in Lake Ontario are used to evaluate the performance of circulation models for different time scales. The measurements were taken in a single cross-section of the lake with sufficiently high resolutions to verify mass balance requirements for water transports through the section. The results indicate that a typical hydrodynamic model can reproduce short- and medium-term circulations induced by wind variations but may be unable to simulate long-term climatic current patterns.

The results of this study are particularly useful to update the climatology of lake circulation needed for the transport and distribution of toxic contaminants and water quality parameters. This paper has

. . . . 2

been submitted for publication in the Journal of Physical Oceanography since the conclusions are equally interesting to the Limnological and Oceanographic scientific community.

RÉSUMÉ ADMINISTRATIF

Les modèles hydrodynamique semblent être généralement acceptés comme des outils valables permettant de déterminer la dynamique de la circulation dans les lacs et les océans et de simuler à court terme la configuration des courants locaux et les transports de masse d'origine climatique dans ces milieux. Contrairement aux modèles météorologiques, qui sont constamment mis à jour grâce aux observations régulières effectuées dans un grand nombre de stations météorologiques, les modèles de la circulation océanique ne peuvent être contrôlés adéquatement à partir de la base de données existante, de sorte que l'évaluation de leur performance est plutôt subjective. Néanmoins, des vérifications systématiques des modèles hydrodynamiques de la circulation dans les Grand Lacs, même si elles soulèvent de sérieux doutes sur leur pouvoir de simulation à long terme, n'ont pas réussi à modifier ce préjugé favorable. On estime peut-être que les différences entre les échelles océanique et limnologique ou entre les processus dynamiques empêchent toute comparaison des modèles de la circulation dans les lacs et les océans.

De longues séries chronologiques d'observations courantométriques dans le lac Ontario permettent d'évaluer la performance des modèles de circulation à différentes échelles temporelles. Des mesures ont été prises le long d'un profil du lac avec suffisamment de précision pour déterminer le bilan de masse nécessaire au transport de masses d'eau à l'endroit considéré. Les

résultats révèlent qu'un modèle hydrodynamique type peut reproduire à court et à moyen terme la circulation due aux variations des vents, mais qu'il ne peut simuler à long terms la configuration des courants dus aux variations climatiques.

Les résultats de ces travaux sont particulièrement utiles pour l'étude de la qualité de l'eau et des facteurs climatiques influant sur la configuration de la circulation dont dépendent le transport et la distribution des polluants toxiques. Ce rapport a été envoyé au Journal of Physical Oceanography pour publication car les conclusions de l'étude peuvent également intéresser les limnologues et les océanologues.

ABSTRACT

Current meter observations in Lake Ontario covering the 140-day period from 4 November 1982 to 23 March 1983, are used to evaluate the performance of circulation models for different time scales. The measurements were taken in a single cross-section of the lake with sufficiently high resolution to verify mass balance requirements for water transports through the section. The results indicate that a typical hydrodynamic model can reproduce short- and medium-term circulations induced by wind variations but may be unable to simulate long-term climatic current patterns.

RÉSUMÉ

Des observations courantométriques ont été effectuées dans le lac Ontario sur une période de 140 jours, du 4 novembre 1982 au 23 mars 1983, pour évaluer la performance de modèles de la circulation à différentes échelles temporelles. Les mesurer ont été prises le long d'un profil du lac avec suffisamment de précision pour déterminer le bilan de masse nécessaire au transport de l'eau à l'endroit considéré. Les résultats révèlent qu'un modèle hydrodynamique type peut reproduire à court et à long terme la circulation due aux variations des vents, mais qu'il ne peut simuler à long terme la configuration des courants dus aux variations climatiques.

1. INTRODUCTION

Hydrodynamic models appear to have been generally accepted as useful tools to elucidate the dynamics of ocean circulations and to simulate short-term local current patterns as well as climatological mass transports in the world's oceans. Unlike their meteorological counterparts which have been constantly improved by recourse to routine observations from a dense network of weather stations, oceanic circulation models cannot be adequately verified with the available data base and their acceptance is based more on faith than fact. There is no indication that this faith has been shaken by the conclusions of systematic verification studies of hydrodynamic models of the Great Lakes which raise serious doubts about the ability of such models to simulate long-term circulation patterns (Simons, 1976; Allender, 1977; Bennett, 1977; Schwab, 1983). Perhaps it is felt that the disparity of oceanic and limnological scales or differences in dynamical processes render a comparison of circulation models of lakes and oceans invalid.

The dynamics of lakes and oceans may be contrasted by recourse to the vorticity balance for the vertically-integrated mass transport or, more specifically, the vorticity equation for the vertically-averaged transport

$$\frac{\partial}{\partial t} \nabla \cdot \left(\frac{\nabla\psi}{H}\right) = J\left(\frac{f}{H}, \psi\right) - \nabla \cdot \left(\frac{B}{H} \nabla\psi\right) + \text{curl}\left(\frac{\tau_s}{H}\right) \qquad (1)$$

where t is time, ψ the mass transport stream function, H the depth, f the Coriolis parameter, ∇ the horizontal gradient operator, J the Jacobian, τ_s the wind stress, B a depth-dependent bottom stress coefficient and effects of baroclinic pressures and nonlinear accelerations have been ignored. The first term on the right represents planetary and topographic vorticity tendencies. While the beta-effect is generally predominant in the oceans, the Coriolis parameter may be treated as a constant in lake models with the result that the topographic effect takes over. Thus, the planetary Rossby waves of ocean models are replaced by topographic normal modes in lake models. The last term on the right is similarly affected by the spatial scales of oceans and lakes. While large-scale ocean circulations are governed by the curl of the wind, the dimensions of lakes are small compared to typical weather systems and hence the wind stress is in first approximation uniform. As pointed out in studies of the North Sea (Groen and Groves, 1962), shelf waves (Gill and Schumann, 1974), and lakes (Bennett, 1974), such smaller-scale circulations are generated by depth gradients normal to the wind. Finally, the bottom stress coefficient as determined from Ekman theory is proportional to the inverse of the depth in deep water but tends to become inversely proportional to the square of the depth in shallow water (Simons, 1983; Schwab, 1983).

There may also be some doubt whether, in spite of the extensive data base used in circulation studies of the Great Lakes, the spatial resolution of the measurements has been adequate for model verification. The common procedure in these studies has been to more or less cover the basin with a network of current meters and to compare observations with model results in adjacent grid points. It would clearly be preferable to design a measurement array which permits unambiguous interpolation between instruments such that mass conservation requirements are satisfied. Thus, rather than a sparse network of stations for the whole lake, one might choose a high-resolution array of instruments in one or more cross-sections. Such an experiment was carried out in Lake Ontario in the winter of 1982/1983 with the goal of evaluating the performance of typical lake circulation models and by extension, obtaining an indication of the reliability of similar ocean models.

The simulation capability of a circulation model will likely depend on the time scales under consideration and on the relative importance of various dynamical processes in a given situation. Indeed, results of past experiments show that the immediate response of a lake to a strong wind impulse is more readily simulated than long-term circulations dominated by frictional effects or stratification (Simons, 1980). In view of this, the following analysis considers short-term and long-term circulations separately.

2. OBSERVATIONS

From 4 November 1982 to 23 March 1983, two arrays of self-recording current meters were operated in Lake Ontario, the first one following the 50 m depth contour along the northshore, the second one extending across the lake from Port Hope, Ontario to Point Breeze, New York (Fig. 1, top). Current meters were placed at depths of 12 m below the surface, 1 m above the bottom, and at the 50 m level in deep moorings. A total of 34 complete records were obtained from the 140-day period of measurement. Data from the alongshore array have been presented by Simons (1984) to illustrate effects of topographic waves on wind-driven coastal currents. The present study is based on the cross-lake observations (Fig. 1, bottom).

Winds are available from routine weather observations at Toronto Island Airport, slightly west of Station A7. During the first 80 days of the experiment winds were also measured by a meteorological buoy at Station C7 and by shore-based wind recorders at both ends of the cross-lake array. The wind records from the buoy were frequently interrupted by icing problems and hence are not very usefull. Frequency spectra of wind records from the two shore stations have the same shape as the Toronto Island wind spectrum but the amplitudes are reduced by height differences and, perhaps, some sheltering effects. Earlier measurements taken by a similar wind recorder on the beach

near the Toronto Island weather station showed a uniform reduction of the wind spectrum for periods longer than a few days. If this result is used to adjust the present shore-based measurements, the wind at the southshore station becomes almost identical in speed and direction to that on Toronto Island when averaged over the common period of operation. At the northshore station the mean wind speed is 15% lower and the direction is turned 40 degrees counterclockwise.

Since the Toronto Island wind record is continuous and appears to be quite representative of wind conditions over the lake, it is used for the present calculations. The wind is taken to be uniform but the possible effects of a long-term windshear as observed between the two shore-based wind recorders will be evaluated. The wind stress is obtained from the square of the windspeed with a drag coefficient ranging from 1.5×10^{-3} for windspeeds less than 10 m s^{-1} to 3.0×10^{-3} for speeds over 20 m s^{-1} with a linear variation in between. These relatively high values are suggested by earlier model studies of the Great Lakes (Simons, 1975; Schwab, 1978) and, again in this study, appear necessary to reproduce observed short-term current variations.

Currents are decomposed into alongshore and onshore components, the alongshore direction being normal to the cross-lake measurement array. The model verification is concerned exclusively

with water transports through the cross-section, i.e., with alongshore currents, since these measurements can be checked for mass conservation. All records are low-pass filtered to remove short-term oscillations due to free surface waves, seiches, tides and inertial motions. The amplitude response of the digital filter decreases from unity for periods longer than 24 hours to zero for periods shorter than 18 hours.

Current fluctuations are found to be highly correlated in the vertical, even in the deepest stations, as expected under homogeneous conditions. Amplitude reduction of bottom currents is consistent from one station to the next. The ratio of standard deviations of surface and bottom currents ranges from 1.2 to 1.4. In view of this vertical consistency of the measurements, reliable estimates of vertically-integrated mass transport may be obtained by simple linear interpolation between instrument depths. For moorings C_1, C_{10} and C_{11}, current records are available for a single depth only (see Fig. 1). For the purpose of computing mass transports, the missing currents are obtained by using the ratio of standard deviations of surface and bottom currents in adjacent stations. Vertically-averaged currents used in the present study are defined as vertically-integrated transports divided by depth.

3. NUMERICAL MODELS

Choosing the most suitable model for studies of this kind is not a straightforward matter. There is a choice of free surface or rigid lid models, vertically-integrated or multi-level formulations, various finite-difference lattices or some other spatial discretization. The present study is not directed at a comparison of different modeling techniques. Instead, the primary intent is to see if conventional and representative hydrodynamic models are capable of simulating the main characteristics of observed circulation patterns. For a homogeneous basin the most direct approach is to solve the vertically-integrated equations of motion and the continuity equation on a single Richardson lattice or, if divergence effects are suppressed by the rigid lid approximation, to solve the vorticity equation (1) on a rectangular grid.

The rigid lid approximation rests on the assumption that the characteristic length scales are smaller than the ratio of the surface wave speed to the Coriolis parameter. With a typical depth of 100 m and a basin width well below 100 km, topographic circulations in Lake Ontario are unlikely to be affected by free surface effects and hence the vorticity equation should give the same solutions as the shallow water equations. However, allowance must be made for numerical truncation errors caused by imperfect resolution of finite difference

schemes. Since such errors may be quite different for the rigid lid and free surface models, it appears worthwhile to use both of them for the present simulations. Also, effects of model resolution will be explored in the next section before proceeding to the actual model calculations for Lake Ontario.

The vorticity equation for the rigid lid model has been presented in the Introduction. The equivalent free surface equations are

$$\frac{\partial U}{\partial t} = -gH \frac{\partial h}{\partial x} + fV - BU + \frac{\tau_{sx}}{\rho} \tag{2}$$

$$\frac{\partial V}{\partial t} = -gH \frac{\partial h}{\partial y} - fU - BV + \frac{\tau_{sy}}{\rho} \tag{3}$$

$$\frac{\partial h}{\partial t} = -\frac{\partial U}{\partial x} - \frac{\partial V}{\partial y} \tag{4}$$

where U, V are the components of the vertically-integrated transport vector in x, y direction, h is the free surface displacement, g is gravity, ρ is density and the notation is otherwise the same as in equation (1). Based on model studies of the Great Lakes (Simons, 1983; Schwab, 1983) the best estimate of the bottom stress coefficient is $B = 5 \times 10^{-3} H^{-2}$ where H is expressed in meters and B has

dimensions of s^{-1}. The corresponding frictional time scale varies from one day for depths of 20 m to 100 days for depths of 200 m, a typical overall value for Lake Ontario being 10 days.

On a single Richardson lattice, the model variables are staggered in space with the surface elevation being defined at the centre of a grid square and the normal components of the transport vector on the sides of the square. Spatial derivatives are approximated by central differences and the Coriolis term is obtained by averaging over four surrounding points. In order to preserve total kinetic energy in the averaging process, the Coriolis terms in (2) and (3) are multiplied by $(1 + H_u/H_v)/2$ and $(1 + H_v/H_u)/2$, respectively, where H_u and H_v are the depths in u- and v-points, respectively. Time extrapolation is carried out by applying a single-step forward scheme to each variable in turn, thereby using the most recent values of the two other variables. Due to the structure of the equations this procedure is equivalent to a forward-backward scheme for the Coriolis terms and a leapfrog scheme for the pressure-divergence terms, with the time step being determined by the CFL condition (see e.g., Simons, 1980). The present Lake Ontario model employs a mesh size of 5 km and a time step of 75 s.

The solution of the vorticity equation also employs a single-step scheme for time extrapolation and central differences for

spatial derivatives. The Coriolis term is averaged over the old and new time step and hence appears on the left as well as the right hand side of the finite difference equation. The frictional term is evaluated forward in time which sets an upper bound on the time step in shallow water. The time step used for the Lake Ontario calculations was one hour. Solutions were obtained by relaxation with an overrelaxation factor of 1.5. In order to achieve convergence of long-term mean solutions it was found necessary to continue the iteration process until the difference between successive iterations was everywhere smaller than 1 $m^3\ s^{-1}$, while typical instantaneous values of the stream function were of order $10^5\ m^3\ s^{-1}$. The number of required iterations is considerably reduced if the first guess is obtained by linear extrapolation from the last two time steps.

4. MODEL RESOLUTION

Since wind-driven circulations in homogeneous lakes are dominated by topography, the required resolution of a numerical model is essentially determined by the maximum depth gradients encountered in the basin. In Lake Ontario (Fig. 1) the southshore bottom slope is twice as steep as the northshore slope and hence numerical truncation errors may be anticipated to be most severe along the southern shore. A straightforward method of evaluating such truncation errors is to

increase the model resolution until the solution converges. It is not practical to apply this procedure to the actual lake since studies of topographic waves suggest that the grid spacing should be less than 1 km which translates into 10^4 - 10^5 grid points for the whole lake. As an alternative, the procedure was applied to an idealized basin with topographic features similar to Lake Ontario.

An idealized basin which has received a great deal of attention in theoretical studies is the circular basin with parabolic depth profile. Analytical solutions are available for the inviscid, time-dependent response to a wind impulse (Birchfield and Hickie, 1977) as well as steady state circulations (Birchfield, 1967, 1973). The first step of the present resolution experiments was to extend these solutions to include bottom friction in time-dependent problems and to allow for more realistic depth variations. This was done by applying the method of separation of variables to reduce the two-dimensional problem to a one-dimensional problem which can be solved numerically with sufficient resolution to assure that the solutions are exact. The second step was to solve the same problem on a two-dimensional rectangular grid with lower resolution and to compare the results with the exact solutions.

The one-dimensional problem is formulated by assuming that the depth of the circular basin is a function of radius only and by

writing the dynamical equations (1) - (4) in polar coordinates. For a uniform wind, the wind stress components in these equations are proportional to the sine and cosine of the azimuthal angle and hence the solutions must be of the same form. Substituting such solutions leads to equations in which the radius of the basin appears as the only spatial variable. The corresponding finite-difference equations were formulated for the free surface as well as the rigid lid model. In this case, the vorticity equation can be solved conveniently by direct matrix inversion.

When applied to problems of inviscid circulation in circular basins with parabolic depth profile, both one-dimensional numerical models were found to converge to the available analytical solutions. The parabolic depth was then replaced by the steep southern slope of the depth profile of Lake Ontario shown in Fig. 1. Since the width of this slope region is about 20 km, an interior region of constant depth was added such that the diameter of the circular basin was comparable to the width of the cross-section of Fig. 1. With bottom friction included, both numerical models were run with increasing resolution until their solutions converged. These results will be referred to as the exact solutions. As expected, the models required a grid spacing less than 1 km to reduce the errors to a few percent of the currents. This grid interval represents a few percent of the width of the bottom slope region.

Two examples of the resolution experiments will be presented here because they have a direct bearing on the following discussion of Lake Ontario calculations. The first one concerns the response to a wind impulse of finite duration, the second one is the long-term averaged current induced by actual winds observed during the 1982/1983 Lake Ontario experiment. In each case the model solution of interest is the current in the diameter perpendicular to the wind.

Figure 2 presents the impulse response as a function of offshore distance and depth. The solid lines represent the exact solutions obtained from the high-resolution one-dimensional models. The dashed curves show results from a free surface model with a two-dimensional rectangular grid with resolution of 5 km. The dotted lines present results from a two-dimensional rigid lid model with the same grid spacing. For this particular problem, the 5 km resolution appears acceptable for the free surface model but not for the rigid lid version. If the grid spacing of the latter is reduced by one half, the accuracy becomes comparable to that of the former.

Figure 3 compares long-term results obtained by forcing the circular basin with winds observed on Lake Ontario during the 140-day period from 4 November 1982 to 23 March 1983. The solutions on the left were averaged over the first 70 days, the results on the right are averages for the whole period. Since the mean wind over the

second half of the experiment is opposite to that of the first half, the net wind and, hence, the net circulation is very small. Again, the solid lines present the exact solutions. The squares represent the free surface model with a two-dimensional grid of 5 km, the circles show results from the two-dimensional vorticity model with a grid of 2.5 km. For the low bottom friction used in the present studies, the free surface model tends to overestimate topographic current oscillations in deep water. This leads to serious errors when solutions are averaged over long periods of time, especially if the mean forcing tends to vanish.

5. SHORT-TERM CURRENT FLUCTUATIONS

The short-term model performance is, in this study, evaluated by comparing the response of the model and the real lake, respectively, to a finite wind impulse. Impulse response functions are familiar from storm surge prediction (Schwab, 1978) and have also been used for computing wind-driven coastal currents (Simons, 1984). For the hydrodynamic model, the response characteristics are determined by forcing the model with a unit wind impulse and recording the time variations of computed currents in grid points of interest. For the lake itself, empirical response functions can be obtained from observed current series provided that simultaneous wind records are available.

The impulse response method becomes particularly simple if the basin is of small extent compared to typical weather systems such that the wind field may be assumed to be uniform over the whole lake. In that case the current, u, at a particular location can be written as

$$u(t) = \int_0^T \tau\,(t - t') \cdot R\,(t')\,dt' \qquad (5)$$

where τ is the wind stress history, R the impulse response function for the location of interest and T represents the finite memory of the lake due to friction. In terms of observations at discrete time intervals, Δt, and memory $N = T/\Delta t$, equation (5) becomes

$$U_i = \sum_{n=1}^{N} \tau_{i-n} \cdot R_n \qquad (6)$$

Given a wind and current record, equation (6) generates a system of equations which can be solved for the unknown impulse response. In order to obtain reliable results, the length of the data series must be much greater than the length of the response function and the system must be solved by a least squares algorithm. After some experimentation, a suitable time step was found to be 12 hours with winds and currents being staggered in time. To utilize the

complete current records, the wind record was extended backward in time.

While the water transports through a north-south cross-section of the lake are most likely dominated by the east-west component of the wind, effects of the north-south component cannot be ruled out. Thus, the empirical modeling procedure included both components of the wind. The response to the wind component normal to the cross-section shows good convergence for different truncation of the response function between 10 and 30 days but the response to the second wind component does not. Therefore, the short-term model verification is confined to the response of alongshore currents to alongshore winds.

Computation of empirical response functions may be adversely affected by the low-frequency portions of the wind and current spectra. To avoid this problem, long-term oscillations were eliminated by a high-pass digital filter. The separation of time scales is somewhat arbitrary but, clearly, the cut-off period should be longer than the memory of the lake as estimated from the impulse response functions. In this study, long-term current variations are taken to have time scales of one month or longer. The high-pass filter fully preserves fluctuations with periods shorter than 35 days and completely eliminates currents with periods longer than 46 days.

Results of computations are presented in Fig. 4. The solid lines show the empirical current response to a 12-hour wind impulse for all current meter moorings of the cross-lake array of Fig. 1. The sounding depth is shown for each station and the results are ordered from shallow to deep water on both the northern and southern half of the section to illuminate the asymmetry of the response. The broken curves show impulse response functions computed by a 5 km free surface model in corresponding grid points or, for a few stations, in the middle of two adjacent grid points. The correspondence between empirical and computed response is best near the northern shore and in deep water and is particularly poor for stations with depths approaching the mean for the cross-section (100 m).

As noted in the Introduction, the present measurement program was designed to permit unambiguous interpolation between instrument positions and verification of mass balance conditions for water transports through the cross-section of the lake. An objective computer algorithm was used for horizontal interpolation of the vertically-integrated mass transports computed for each station as outlined above. Boundary conditions are zero transport at the shores. The empirical cross-lake distributions of transports generated by a 12-hour wind impulse are presented in the left-hand panel of Fig. 5. Corresponding results from the 5 km free surface model are shown in the right-hand panel. Good agreement is observed during the first few

days and again after the fifth day or so, but considerable differences occur at intermediate times and, in particular, near the mean depth of the cross-section. According to simple models of wind-driven lake circulation (Bennett, 1974), the mean depth contour tends to separate downwind coastal currents from mid-lake return flow. This effect is quite evident in the initial response of the present model as well as the empirical results.

The main advantage of the data presentation in the form of Fig. 5 is that it permits a check of the internal consistency of the current meter observations and the empirically determined response functions. To that end, the mass transports on the left of Fig. 5 are integrated over eastward and westward current regimes separately and compared in the upper part of Fig. 6. The remarkably close balance lends credence to the model verification procedure adopted in this study. Corresponding mass transports obtained from the model are shown in the lower part of Fig. 6, again based on the interpolated results presented on the right of Fig. 5. In this case the source of the imbalance in the total mass transport can be readily identified. It turns out that approximately one-half of the net westward transport after one day is associated with free surface displacements and the other half is due to interpolation. The interpolation tends to underestimate nearshore transports which, at this time, are directed toward the east as seen in Fig. 5.

6. LONG-TERM CIRCULATIONS

The relatively good performance of the model in simulating the immediate response of the lake to wind is not surprising in view of past experience with lake circulation models (Simons, 1980, 1983; Schwab, 1983). However, as noted in the Introduction, less favorable results must be expected for long-term simulations. This problem will be addressed by using the above-mentioned filter to eliminate current fluctuations with periods shorter than about one month.

The first and last few points of a low-pass series cannot be unambiguously determined. If the digital filter is applied to the total length of the record, the original series must be artificially extended on both sides. Since the original data records have relatively large long-term means and trends, reflection of the series at both ends is probably the best approach. This method was compared with extension with zeros and the differences between the resulting low-pass series were found to be essentially confined to the first and last 10 days. Therefore, in order to avoid ambiguity, the low-pass series were truncated at these points. Figure 7 presents the low-pass time series of observed wind stress and current. The days refer to the 140-day period of measurement starting 4 November 1982 and ending 23 March 1983.

Inspection of the left-hand side of Fig. 7 shows that long-term current variations near the northern shore tend to be correlated with the alongshore wind component. The long-term trend of the southshore current (right-hand side of Fig. 7) is somewhat similar but this current is dominated by a strong mean component toward the east. The deep currents run generally against the wind but their variations in time do not show a strong correlation with the wind. Again, a better illustration of these observations is provided by horizontal interpolation of vertically-integrated transports. The resulting variations for time scales of one month or longer are presented in Fig. 8. The most striking feature of the cross-lake distribution of transport is the belt of strong eastward currents extending from the southshore to well beyond the mean depth contour. In contrast to the northshore currents, the southshore current and the deep lake return flow show no clear correlation with wind variations.

The long-term model calculations utilized hourly values of observed winds starting one month before the onset of the field experiment. The model results were then low-pass filtered in the same way as the observed records. Computations were made with a free surface model with a resolution of 5 km and a rigid lid model with grid spacings of 5 km and 2.5 km. None of the model results compare with observations except in the shallow water near the northshore. The general features of all model solutions are alike. Particularly

similar are the results from the 5 km free surface model and the 2.5 km rigid lid model. As an example, Fig. 9 shows results from the free surface model with the friction formula presented under equation (4). In contrast to the broad belts of observed currents (Fig. 8), the computed circulations are characterized by small-scale features. To ensure that the results were not adversely affected by the start-up procedure or by long-term error accumulation, the model was restarted three months earlier. The results were identical.

Since the computed small-scale circulations are concentrated in deep water they may be partly suppressed if the shallow-water friction formulation given under equation (4) is replaced by the conventional deep-water Ekman friction which is inversely proportional to H rather than H^2. Thus the model was rerun with a friction coefficient $B = 1.5 \times 10^{-4}/H$, which is greater than the shallow water formula for depths greater than 35 m. The resulting currents were too fast in the shore zones and the overall circulation patterns remained the same.

Small-scale circulation features can be readily eliminated by some form of horizontal diffusion of momentum. This was done by adding a Laplacian of the transport to equations (2-3) with a coefficient equal to 25 $m^2\ s^{-1}$. For the 5 km grid, the corresponding diffusive time scale is about 10 days. This removes all small-scale

circulations from the low-frequency solutions as shown in Fig. 10. The results agree with theoretical studies of quasi-steady circulation (Birchfield, 1967, 1973) but there is still no agreement with the observed circulation except near the northshore.

In view of the discrepancies between observed and computed low-frequency currents, it is particularly important to verify the internal consistency of the field data by computing total transports through the cross-section of the lake. The total eastward and westward transports corresponding to the interpolated observations of Fig. 8 are presented at the top of Fig. 11. Ideally, the difference between eastward and westward transports should equal the hydraulic transport associated with the Niagara inflow and the St. Lawrence outflow which is approximately 7×10^3 m^3 s^{-1} to the east. The error is seen to be generally of the order of magnitude of the hydraulic flow but not large enough to invalidate the overall circulation patterns displayed in Fig. 8. For comparison, the total eastward transport computed by the free-surface model with and without horizontal diffusion is shown in the lower part of Fig. 11. In the absence of diffusion, the computed transport is remarkably similar to the observed eastward transport although the cross-lake distribution is completely different.

7. DISCUSSION

The foregoing model results are perhaps best illustrated by contrasting observed and computed long-term mean currents and their standard deviations in time. This comparison is presented in Fig. 12. The solid curve on the left presents the vertically-integrated current distribution across the lake averaged over the 140-day period of measurement. The total eastward transport is 70 x 10^3 m^3 s^{-1} and the total westward transport is 66 x 10^3 m^3 s^{-1}, the net transport being 4 x 10^3 m^3 s^{-1} to the east as compared to the actual hydraulic flow of 7 x 10^3 m^3 s^{-1}. The dotted curve and the short dashes show results from the 5 km free surface model with and without diffusion, respectively, and the long dashes show results from the rigid lid model with resolution of 2.5 km. The corresponding standard deviations in time are presented on the right. Unlike the long-term mean current, the cross-lake variations of short-term current variations are simulated reasonably well.

Part of the problem with the long-term solutions is that numerical truncation errors are accentuated when solutions are averaged over long periods of time. However, when the various model results are interpreted in light of the results of the resolution experiments illustrated in Fig. 3, the discrepancies are readily explained. It is seen, then, that the cross-lake profile of the

long-term averaged model solutions is best reflected by the dotted curve on the left of Fig. 12. This is essentially the steady-state solution corresponding to the mean wind stress for the period of measurement (1.1×10^{-2} Nm^{-2} to the east) and the low friction used here. As known from theoretical models and numerical calculations for Lake Ontario (see Simons, 1980 for a review) the cross-lake profile of the solution consists of bands of wind-driven currents along both shores with adjacent bands of return flow and Ekman drift in the interior. In this particular cross-section of Lake Ontario, numerical steady-state solutions for westerly winds are dominated by a large clockwise circulation cell associated with a wide boundary current along the northshore, while the counterclockwise cell along the southshore is quite weak and only a few km wide. This was verified in the present study by steady-state calculations with high resolution.

The above solutions are clearly at variance with the present observations which are dominated by a large cyclonic circulation cell and much stronger mean currents than those computed by the models. Thus, while the resolution of typical lake circulation models is apparently too low to obtain accurate results, it is most unlikely that models with higher resolution would reproduce the cross-lake distribution of the observed transport. This suggests that the dynamical framework of the models may be inadequate and that some of the assumptions incorporated in the models are not justified. Since

effects of stratification can be ruled out by recourse to the vertical homogeneity of temperature and current measurements, the three assumptions that have to be evaluated are (1) the uniformity of wind in space, (2) the linear relation between bottom stress and vertically-averaged current, and (3) the disregard of nonlinear accelerations.

In regard to the spatial distribution of the wind field it was mentioned in the discussion of the data analysis that the wind recorders at both ends of the measurement array indicated a slight cyclonic curl in the mean wind. To investigate this effect, calculations were made for the extreme case of wind increasing linearly from zero on the northshore to the observed value at the southshore. While this was found to give somewhat larger eastward flow along the southshore, the mean circulation was still dominated by the large clockwise cell associated with the northshore boundary current.

The general effect of bottom friction is known. With increasing friction, the steady-state circulation tends to approach that for a long channel with a single broad band of return flow in the center (Simons, 1980, pp. 74-78). As mentioned earlier, the calculations were repeated with the shallow water Ekman formulation replaced by that for deep water which effectively increased effects of

bottom friction. Also, calculations were made with a three-fold increase of the original bottom friction coefficient presented under equation (4). The only effect was to increase the width of the boundary currents by a few km. However, all these formulas are linear and imply that the long-term mean bottom stress is only a function of the long-term mean current. In presence of large oscillatory currents the mean friction might be totally unrelated to the mean flow if a nonlinear stress law were used such as $\tau_b = c_d|v_b|v_b$ where v_b is the bottom current and c_d a nondimensional drag coefficient. Since extensive measurements of bottom currents were made during the field program, the corresponding nonlinear stresses were computed directly from instantaneous observations and then averaged over the whole period of observation. The resultant bottom stress was then divided by the long-term mean current. In stations near the northshore the mean currents tend to vanish and, hence, separate calculations were made for the first and second half of the period and the results were averaged. Figure 13 presents the results for $c_d = 1 \times 10^{-3}$, which is a low estimate for this coefficient. For comparison, the solid curve represents the shallow water Ekman formula $\tau_b = BH\bar{v}$ with $B = 5 \times 10^{-3}\ H^{-2}$ as used in (1)-(4) and with the bar denoting the vertical-mean current. From the viewpoint of the effects of bottom friction on long-term averaged circulations, the two formulations appear consistent.

The nonlinear accelerations in the alongshore momentum equation are of the form

$$\bar{u}\ \partial\bar{u}/\partial x + \bar{v}\ \partial\bar{u}/\partial y$$

where x and y are the coordinates normal to and along the cross-section. When averaged over time, these terms lead to advection of long-term mean currents and stresses due to correlations of short-term currents. These effects can be estimated from observations in a single cross-section if depth gradients normal to the section are small and the rigid lid approximation holds such that

$$H\bar{u}\ \partial\bar{u}/\partial x = \bar{u}\ \partial(H\bar{u})/\partial x = -\bar{u}\ \partial(H\bar{v})/\partial y$$

The nonlinear terms were computed from daily observations and then averaged over the whole period of measurement. The equivalent stresses (including the advection terms) were found to be eastward in a broad band centered 20 km from the northshore and westward in a 10 km band along the southshore with maximum values comparable to the mean wind stress. While this suggests that nonlinear accelerations are not negligible, their effects in the present case would be to increase the discrepancies between observed and computed long-term circulations.

8. CONCLUSIONS

From the foregoing it appears that neither numerical truncation errors nor simplifying assumptions introduced into the models can explain the disagreement between observed and computed long-term mean circulations. Unlike the typical solutions known from other analytical and numerical studies and computed by the present models, the observations indicate a single circulation cell with the current reversal coinciding with the maximum depth of the cross-section (Fig. 1). Thus, the current pattern is more consistent with a steady vortex of geostrophic flow along closed depth contours. Indeed, a formula of the form $\psi = -KH^2$ with $K = 2$ m s^{-1} and H being the depth profile of Fig. 1, gives a transport distribution very similar to the observed long-term mean except near the northshore. This would suggest that this circulation cell is a remnant of a stratified summer circulation which has been modified by frictional effects in the shallow northshore water. In support of this viewpoint it may be noted that the cross-lake distribution of the long-term trend of observed currents is consistent with the quasi-steady response to the long-term trend of the wind. In other words, if the long-term mean current is subtracted from Fig. 8, the resulting picture looks much like Fig. 10 and hence it would appear that a steady geostrophic vortex might have been a suitable initial condition for the present model calculations. However, a problem with this approach is that the

frictional time scales corresponding to Fig. 13 are too short to maintain any residual summer circulation throughout the winter season.

In conclusion, the present study confirms that typical hydrodynamical models produce fairly reliable simulations of the response of large lakes to short-term wind impulses and even to low frequency wind variations. However, the ability of such models to compute mean circulations for seasonal or annual time scales remains in doubt.

ACKNOWLEDGEMENTS

J.A. Bull, F.M. Boyce and C.R. Murthy planned and supervised the field program and data processing.

REFERENCES

Allender, J.H., 1977. Comparison of model and observed currents in Lake Michigan. J. Phys. Oceanogr., 7: 711-718.

Bennett, J.R., 1974. On the dynamics of wind-driven lake currents. J. Phys. Oceanogr., 4: 400-414.

_____, 1977. A three-dimensional model of Lake Ontario's summer circulation: I. Comparison with observations. J. Phys. Oceanogr., 7: 591-601.

Birchfield, G.E., 1967. Horizontal transport in a rotating basin of parabolic depth profile. J. Geophys. Res., 72: 6155-6163.

_____, 1973. An Ekman model of coastal currents in a lake or shallow sea. J. Phys. Oceanogr., 3: 419-428.

_____ and B.P. Hickie, 1977. The time-dependent response of a circular basin of variable depth to a wind stress. J. Phys. Oceanogr., 7: 691-701.

Groen, P. and G.W. Groves, 1962. Surges. The Sea, Vol. 1, M.N. Hill (Ed.), Interscience, New York: 611-647.

Gill, A.E. and E.H. Schumann, 1974. The generation of long shelf waves by the wind. J. Phys. Oceanogr., 4: 83-90.

Schwab, D.J., 1978. Simulation and forecasting of Lake Erie storm surges. Mon. Wea. Rev., 106: 1476-1487.

_____, 1983. Numerical simulation of low-frequency current fluctuations in Lake Michigan. J. Phys. Oceanogr., 13: 2213-2224.

Simons, T.J. 1975. Effective wind stress over the Great Lakes derived from long-term numerical model simulations. Atmosphere, 13: 169-179.

_____, 1976. Verification of numerical models of Lake Ontario, III. Long-term heat transports. J. Phys. Oceanogr., 6: 372-378.

_____, 1980. Circulation models of lakes and inland seas. Can. Bull. Fish. Aquat. Sci. 203, Can. Govt. Publ. Centre, Ottawa; 146 p.

_____, 1983. Resonant topographic response of nearshore currents to wind forcing. J. Phys. Oceanogr., 13: 512-523.

_____, 1984. Topographic response of nearshore currents to wind: an empirical model. J. Phys. Oceanogr., 14 (Aug. issue).

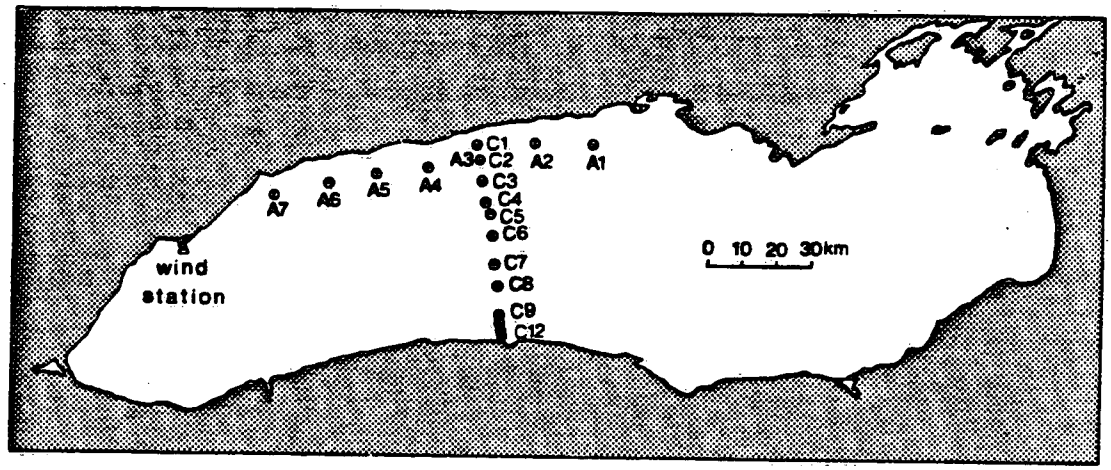

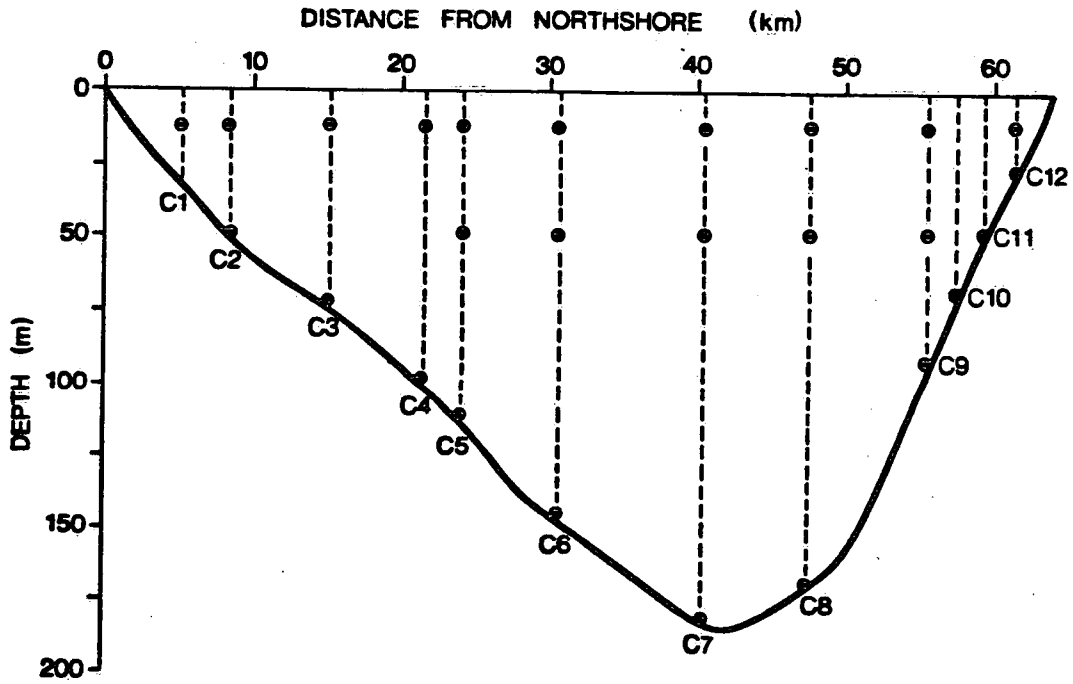

Fig. 1 Location of current meter moorings in Lake Ontario, 4 November 1982 - 23 March 1983 (above) and depth of instruments in cross-lake array (below).

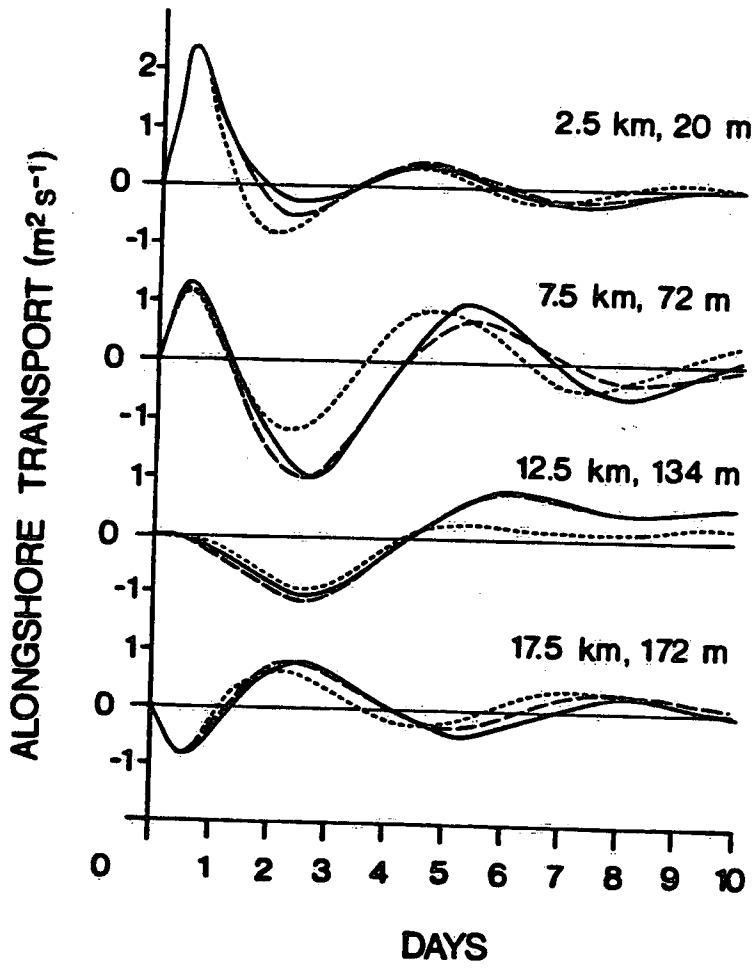

Fig. 2 Response of vertically-integrated currents to 12-hour wind impulse of 10^{-1} Nm^{-2} as a function of offshore distance and depth in a circular basin. Solid: exact solutions; dashed: free-surface model with 5 km grid; dotted: rigid lid model with 5 km grid.

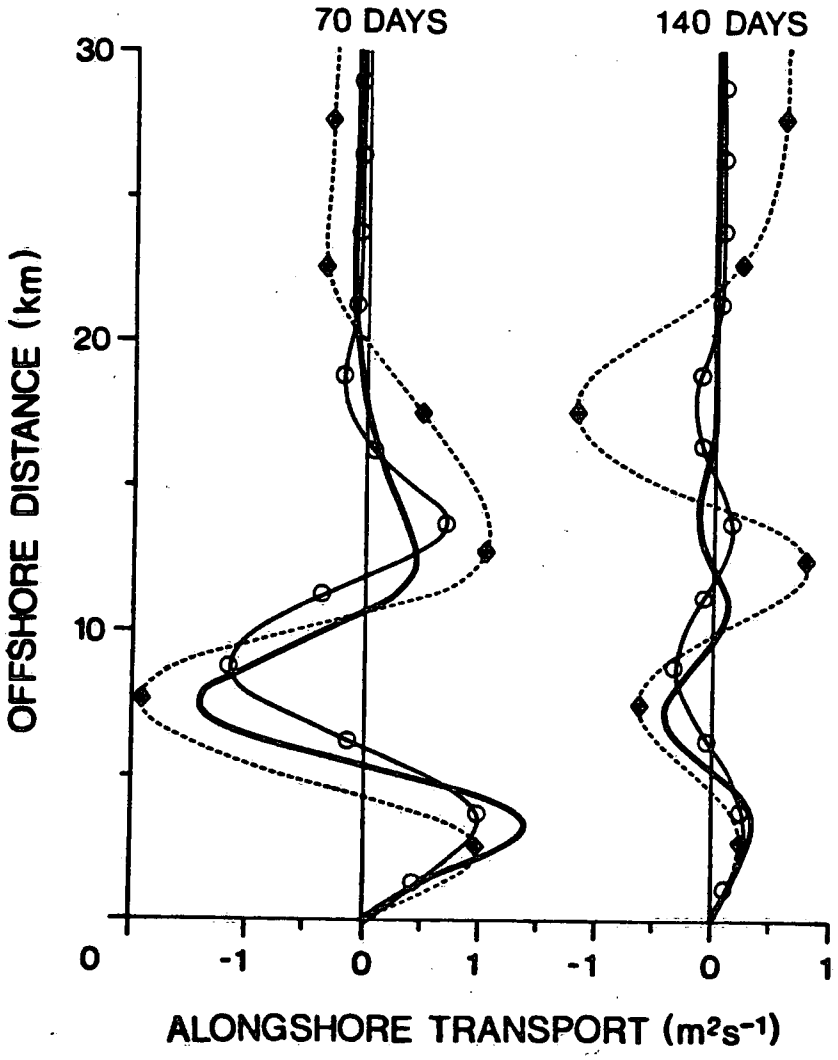

Fig. 3 Long-term means of vertically-integrated currents in a circular basin for winds observed on Lake Ontario, 4 November 1982 to 23 March 1983. Solid lines: exact solutions; squares: free surface model with 5 km grid; circles: rigid lid model with 2.5 km grid.

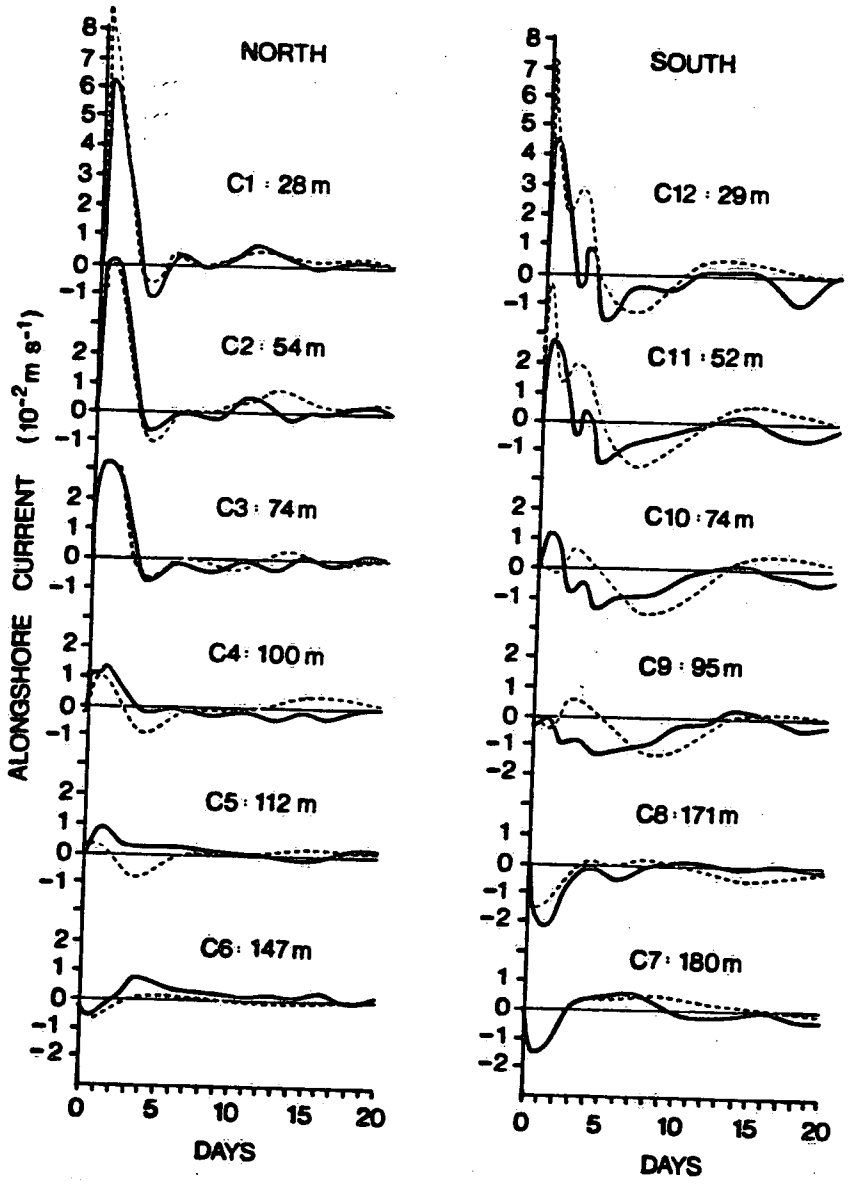

Fig. 4 Response of vertically-averaged alongshore currents to 12-hour wind impulse of 10^{-1} Nm^{-2} for stations of cross-lake array of Fig. 1. Solid curves show empirical results, dashed curves are model results.

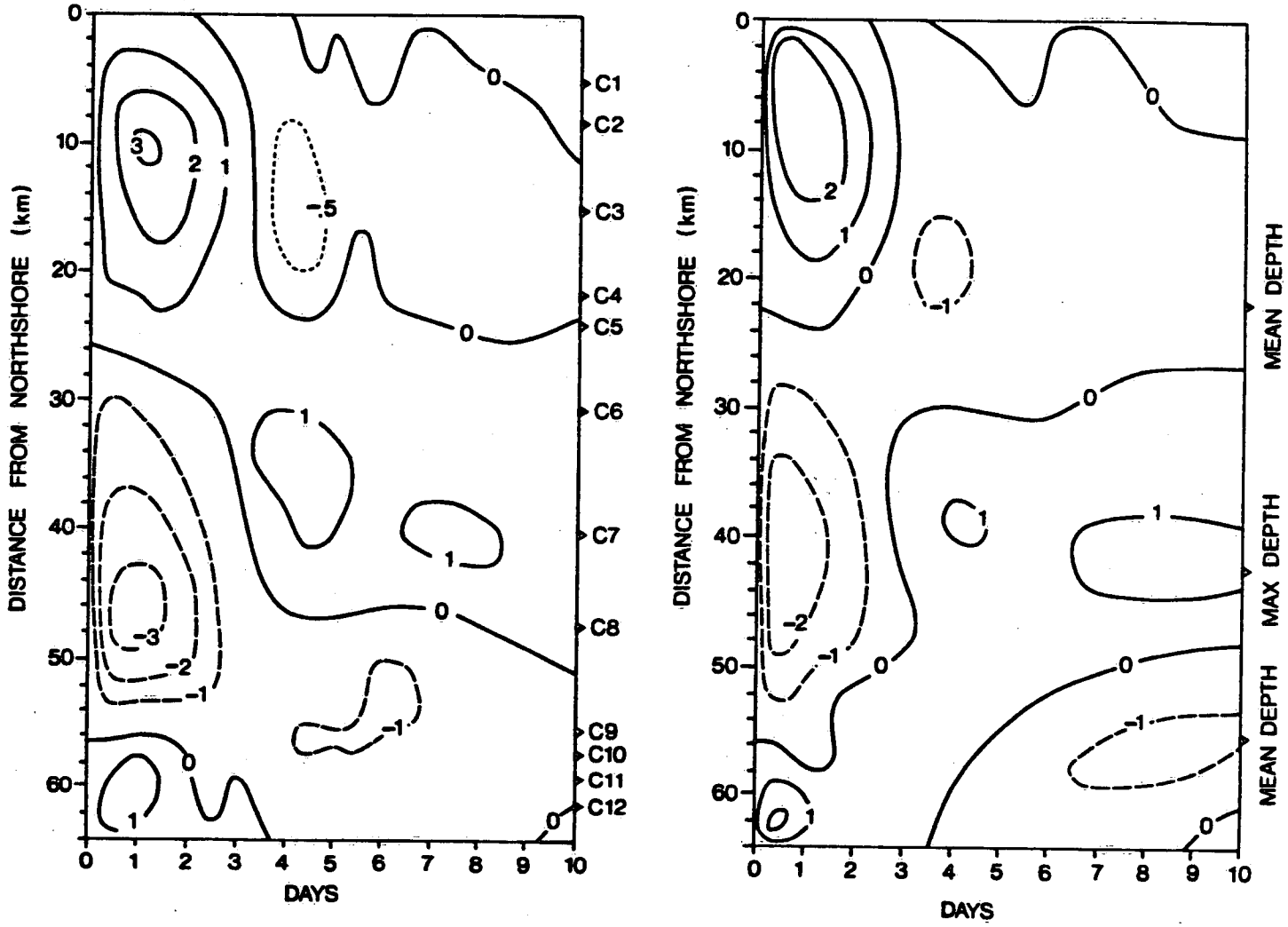

Fig. 5 Cross-lake distribution of vertically-integrated currents (m^2 s^{-1}) corresponding to Fig. 4. Left: empirical results; right: model results.

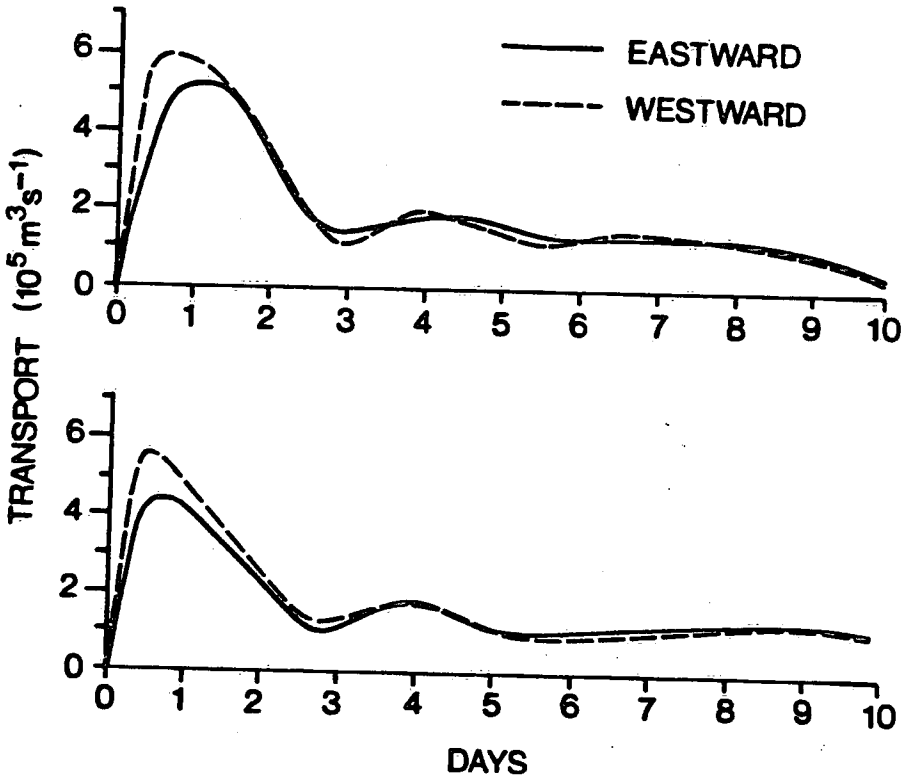

Fig. 6 Total eastward and westward transports corresponding to maps of Fig. 5. Above: empirical results; below: model results.

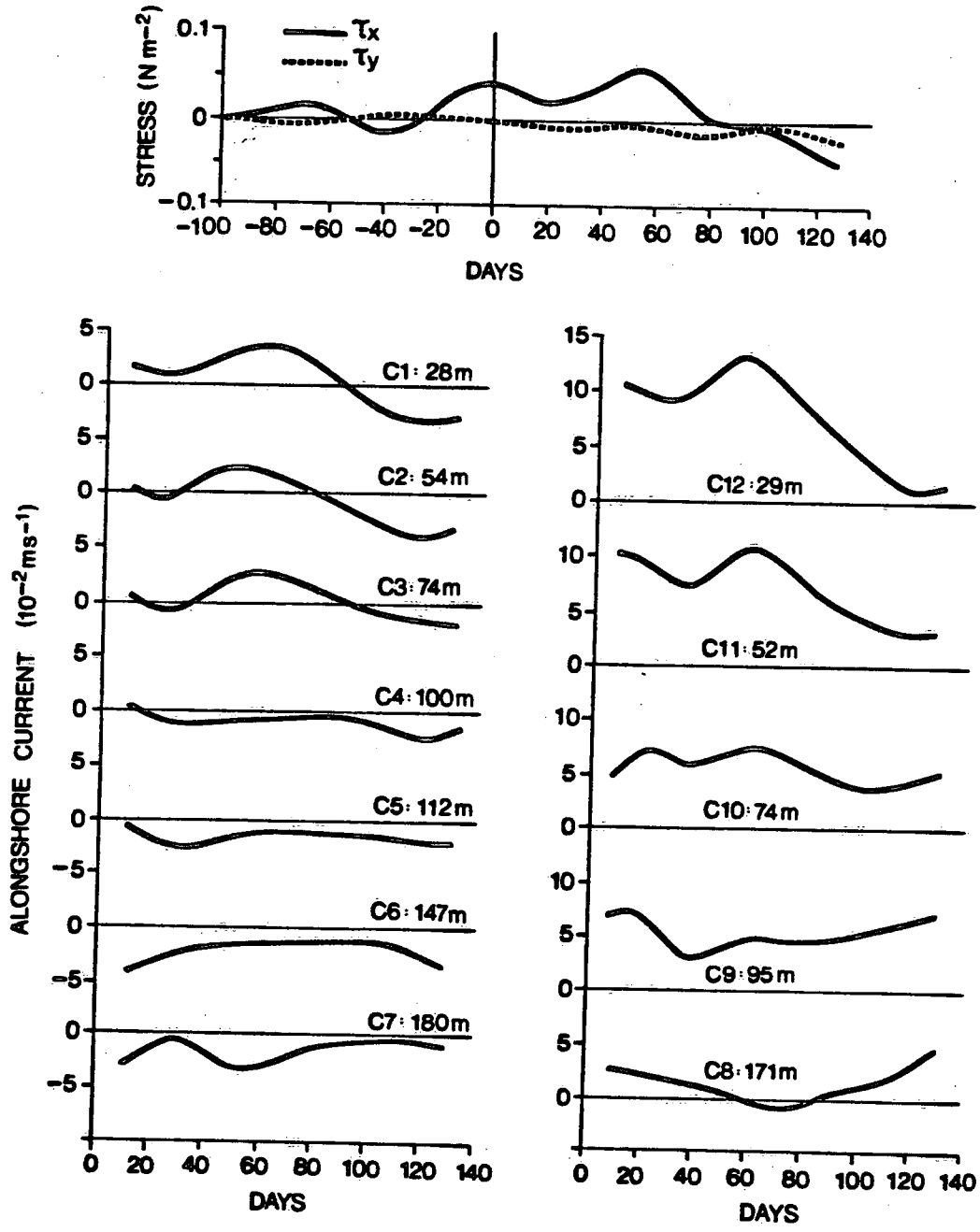

Fig. 7 Low frequency variations of alongshore (τ_x) and onshore (τ_y) wind stress and vertically averaged alongshore currents observed in cross-section of Fig. 1, 4 November 1982 to 23 March 1983.

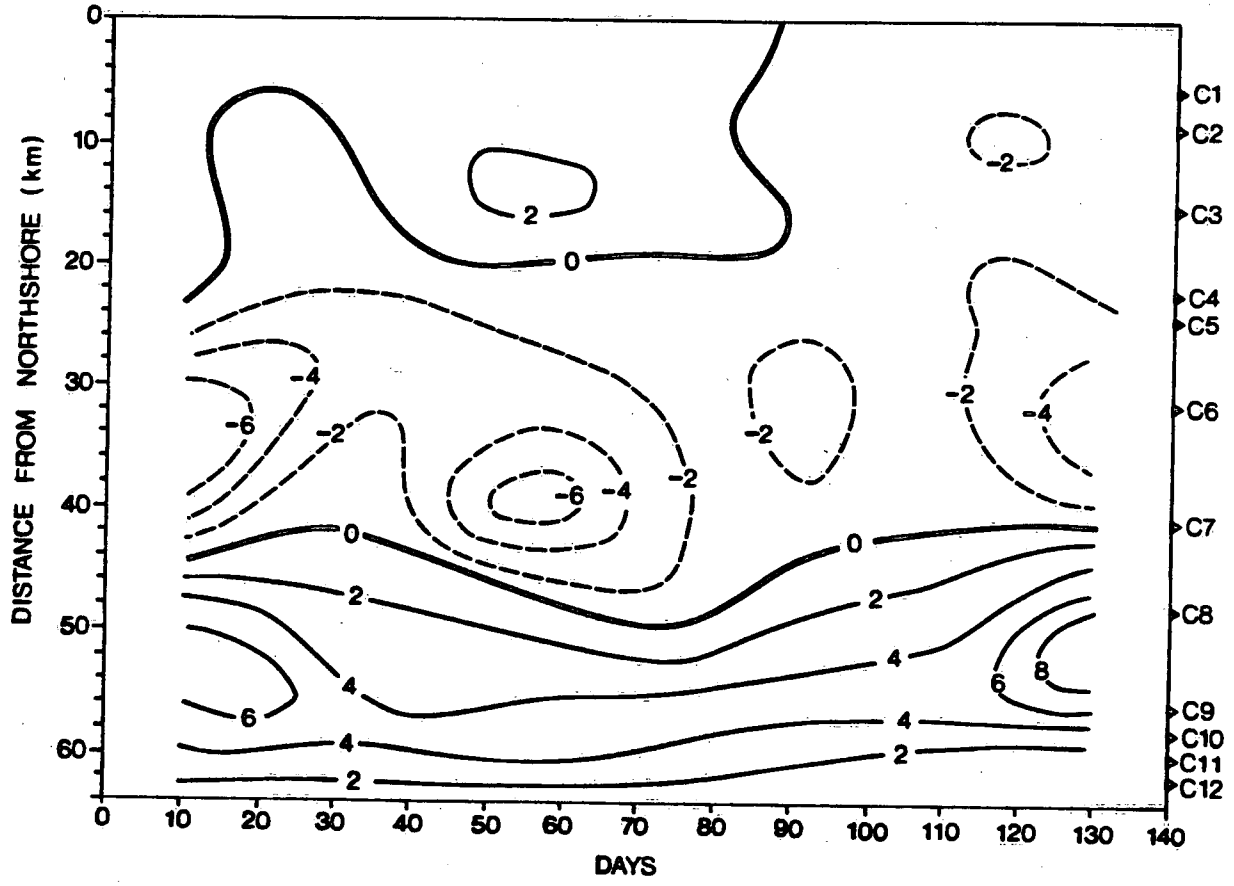

Fig. 8 Cross-lake distribution of vertically-integrated currents ($m^2\ s^{-1}$) corresponding to Fig. 7.

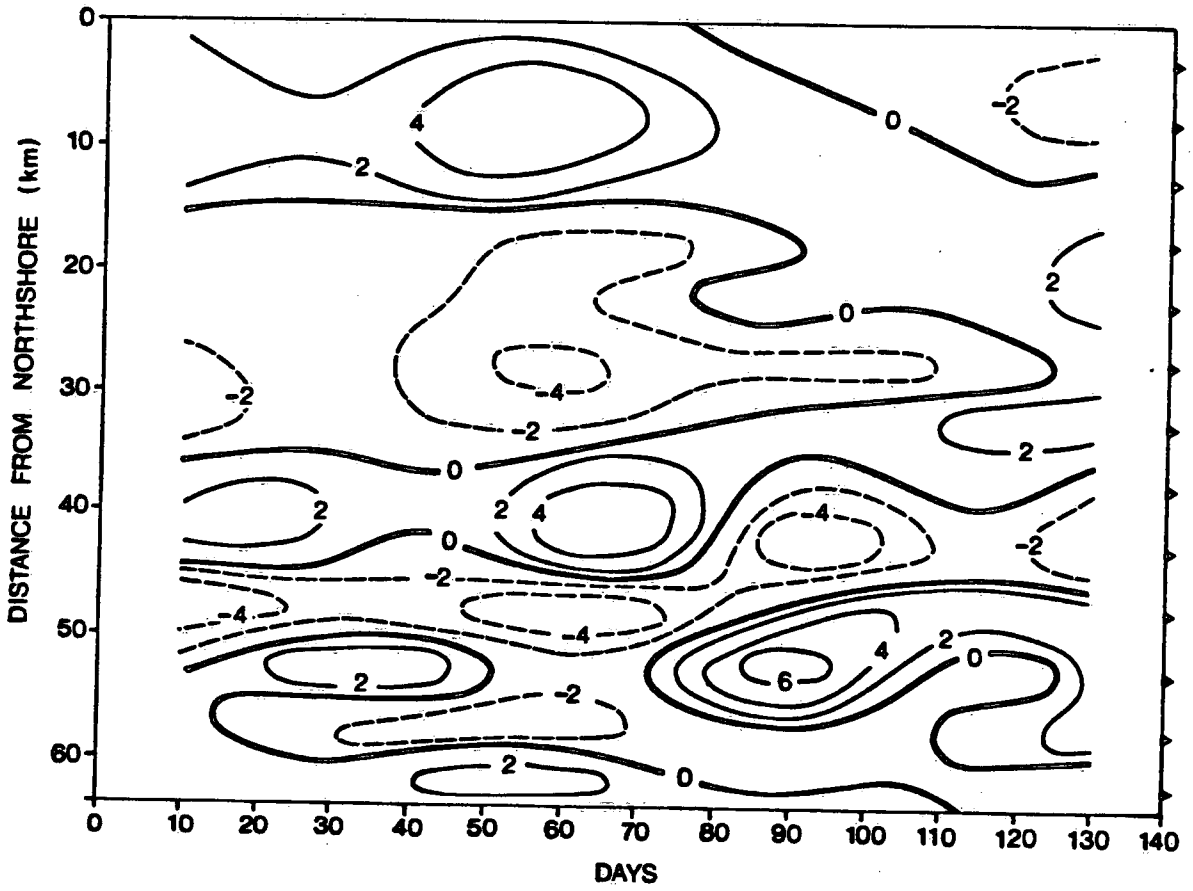

Fig. 9 Cross-lake distribution of low-frequency variations of vertically-integrated currents (m^2 s^{-1}) computed by free-surface model with 5 km grid.

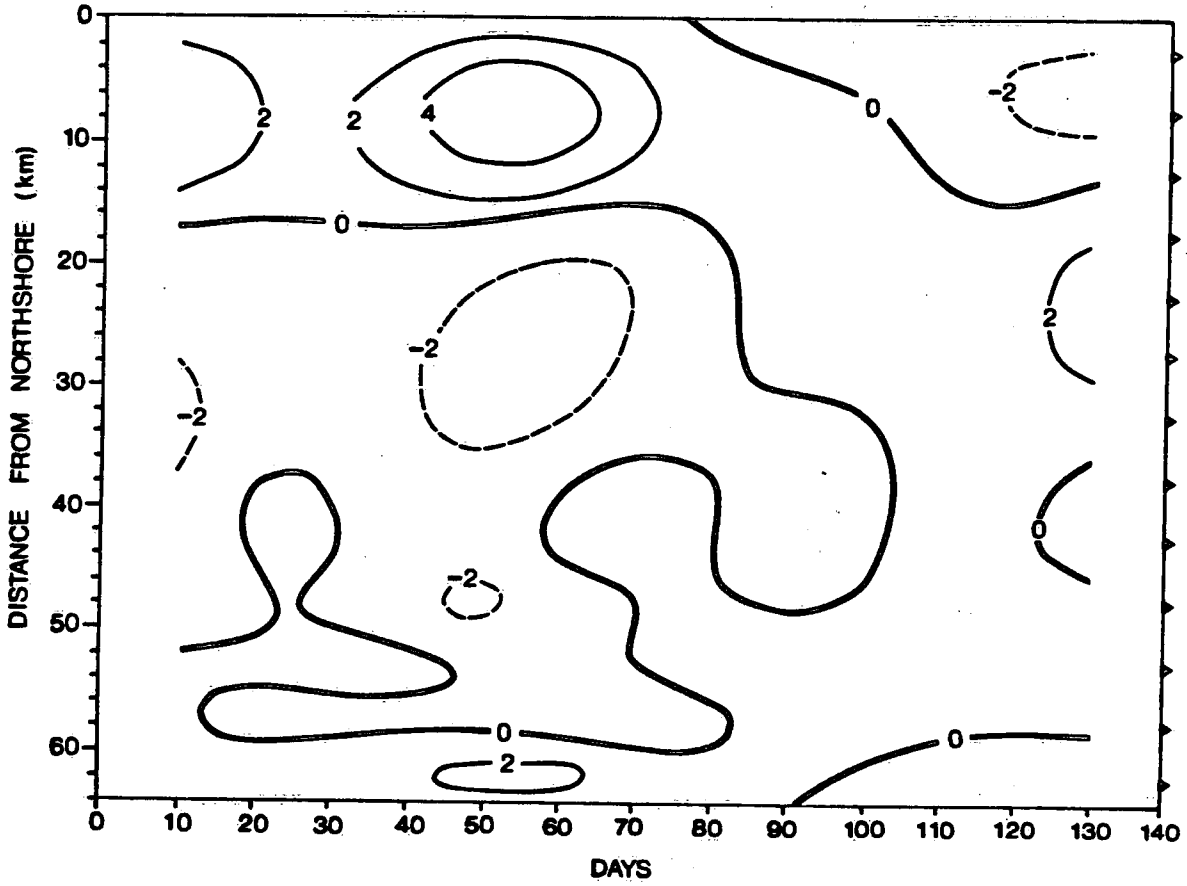

Fig. 10 Same as Fig. 9 but for model with horizontal diffusion of momentum with coefficient of 25 $m^2 s^{-1}$.

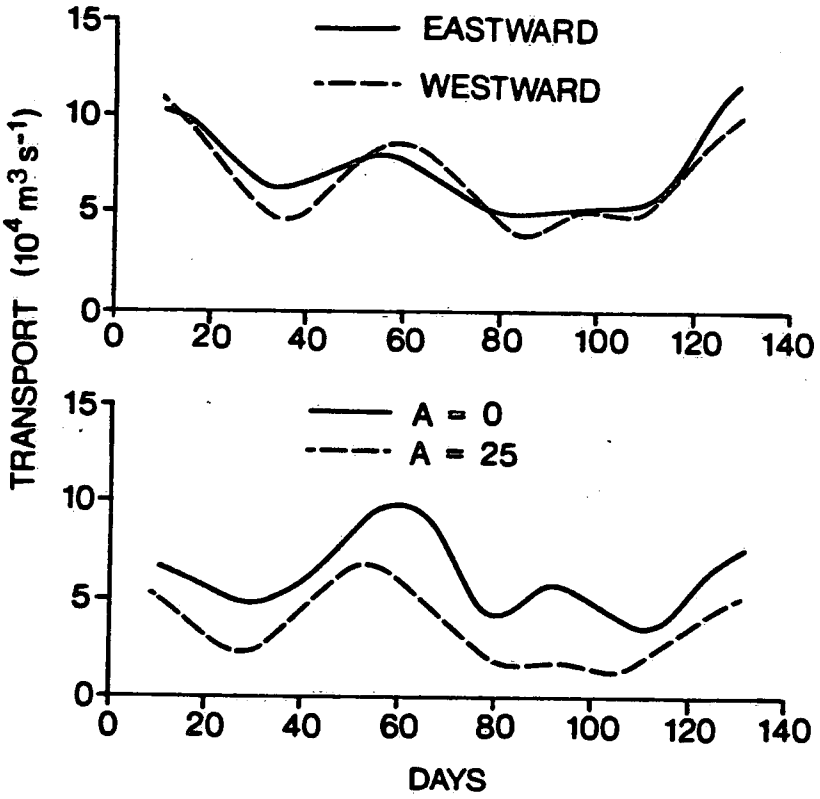

Fig. 11 Above: total eastward (solid) and westward (dashed) transports corresponding to Fig. 7. Below: total eastward transports corresponding to Fig. 9 (solid) and Fig. 10 (dashed).

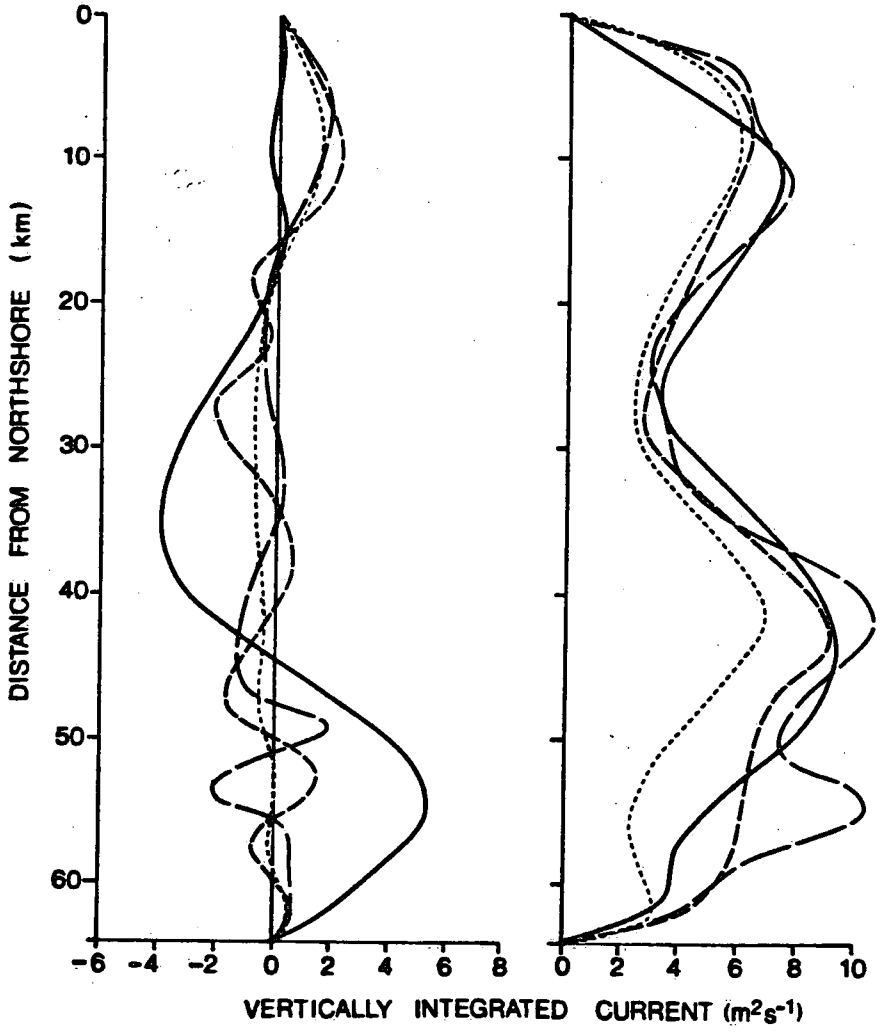

Fig. 12 Long-term means (left) and standard deviations in time (right) of vertically integrated currents for cross-section of Fig. 1, 4 November 1982 to 23 March 1983. Solid: observed; dashed: free-surface model without diffusion; dotted: free-surface model with horizontal diffusion coefficient of 25 m^2 s^{-1}; long dashes: rigid lid model with 2.5 km grid.

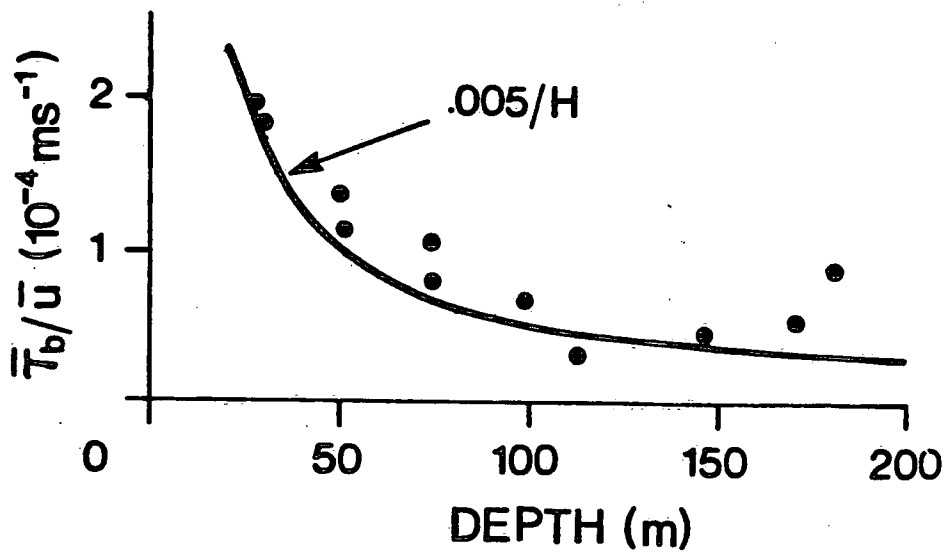

Fig. 13 Long-term mean values of nonlinear bottom stress divided by long-term mean currents as obtained from current meter observations in cross-section of Fig. 1.

9735